

TOTAL CROSS SECTIONS AND ANGULAR DISTRIBUTIONS FOR π^-p CHARGE EXCHANGE
IN THE SECOND AND THIRD RESONANCE REGIONS*†

F. Bulos, R. E. Lanou, A. E. Pifer, A. M. Shapiro, and M. Widgoff
Brown University, Providence, Rhode Island

and

R. Panvini
Brandeis University, Waltham, Massachusetts

and

A. E. Brenner, C. A. Bordner, M. E. Law, E. E. Ronat, K. Strauch, and J. Szymanski
Harvard University, Cambridge, Massachusetts

and

P. Bastien, B. B. Brabson, Y. Eisenberg,‡ B. T. Feld, V. K. Fischer,
I. A. Pless, L. Rosenson, and R. K. Yamamoto
Massachusetts Institute of Technology, Cambridge, Massachusetts

and

G. Calvelli, L. Guerriero, G. A. Salandin, A. Tomasin, L. Ventura, C. Voci, and F. Waldner
Istituto di Fisica dell'Università di Padova, Padova, Italy,
and Istituto Nazionale di Fisica Nucleare, Sezione di Padova, Italy

(Received 3 August 1964)

We have analyzed data at nine different incident pion energies to study the cross sections and angular distributions in the reaction $\pi^- + p \rightarrow \pi^0 + n$. The energies span the region of the second (600 MeV) and third (900 MeV) pion-nucleon resonances. The angular distributions indicate very little structure in the 600-MeV region, but in the 900-MeV region give strong evidence for a $D_{5/2}$ - $F_{5/2}$ interference in the $T = \frac{1}{2}$ state. The data reported here were obtained in a spark-chamber exposure at the Brookhaven Cosmotron designed

to detect the production of neutral final states arising in π^-p collisions. The preliminary charge-exchange angular distributions and cross sections presented herein represent about $\frac{1}{3}$ of the data we will obtain when we have scanned all our film.

A schematic of the experimental setup is shown in Fig. 1. A small liquid hydrogen target, 5 cm in diameter transverse to the beam and 4 cm along the beam, was located inside an anticoincidence shield composed of counters 3 and 5.

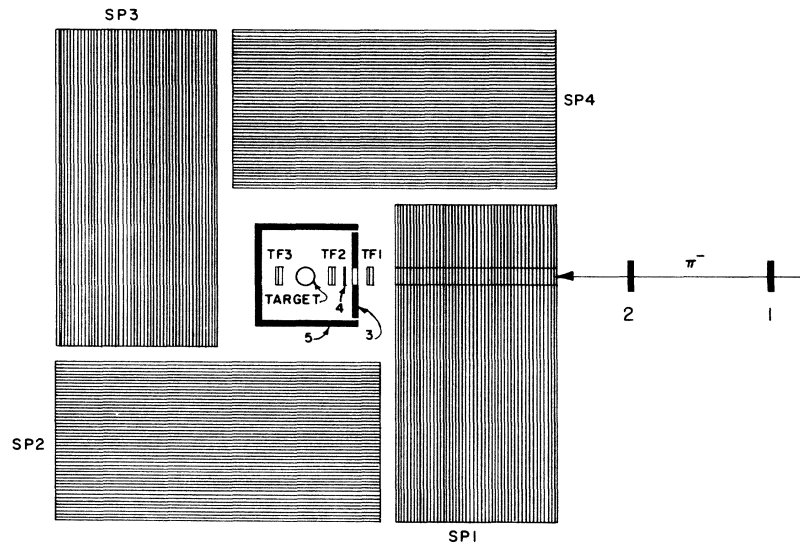


FIG. 1. Experimental setup.

This system was placed inside an array of steel-plate spark chambers,¹ SP1, SP2, SP3, and SP4, each consisting of fifty 2-mm thick plates. The beam was defined by the counter telescope 1 and 2, a 1-inch hole in counter 3, and the $\frac{1}{32}$ -inch thick counter 4. Also included were three thin-foil chambers TF1, TF2, and TF3, which provide information enabling us to reject improper triggers. The rates 1234 and 12345 were recorded and determine the flux and event rate, respectively. The chambers were triggered on the first 12345 signal obtained in each Cosmotron pulse, denoting the disappearance of a beam particle within the anticoincidence shield. Hydrogen-in and hydrogen-out data were taken at 11 energies between 500 and 1100 MeV; data from nine of these energies are represented here.

The photographs were scanned for events with the proper thin-foil chamber signature, TF1, TF2, and TF3, indicating the disappearance of the incoming particle in the target region. About $\frac{2}{3}$ of our hydrogen-in photographs had such a good trigger. The remainder of the photographs contained mainly interactions in SP1, counter 4, or the thin-foil spark chambers, which succeeded in triggering the system. SP1 was provided with thin foils in the beam region to minimize the number of such interactions. Only about $\frac{1}{8}$ of the hydrogen-out photographs contained good triggers. The ratio of beam particles per trigger was about 4:1 for hydrogen-out versus hydrogen-in giving us a signal-to-noise ratio of approximately 15:1. The good-trigger photographs contained any number of gamma-ray showers from 0 to 6. Approximately 90% of the two-gamma events are examples of either of the reactions

$$\pi^- + p \rightarrow \pi^0 + n \rightarrow 2\gamma + n \quad (1)$$

or

$$\pi^- + p \rightarrow \eta^0 + n \rightarrow 2\gamma + n. \quad (2)$$

The remaining 10% are higher multiplicity events such as $2\pi^0$ or $3\pi^0$ production in which only two gammas are seen because our detection solid angle is less than 4π . Reactions (1) and (2) are cleanly separated using the opening-angle technique described in Chretien *et al.*²

The top and bottom of the steel-plate chamber system are open and, therefore, we must calculate an efficiency correction as a function of production angle for our observed events. This was done using Monte Carlo techniques.³

The μ^- beam contamination was determined by calculation, and the e^- contamination was de-

termined, at several energies, by counting the showers initiated by primaries passing through SP3 with the triggering requirement 1234. The former is of the order of 2% and the latter ranges from about $(18 \pm 4)\%$ at 500 MeV to $(7 \pm 4)\%$ at 1000 MeV.

The total cross sections for charge exchange, calculated from the electronic data, the picture

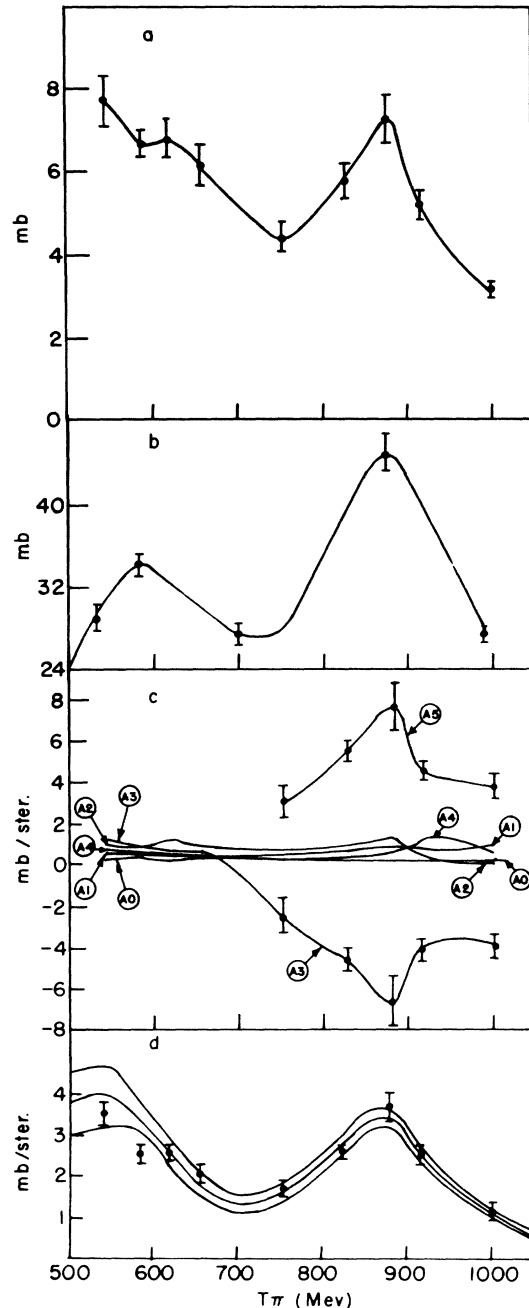


FIG. 2. (a) Charge-exchange cross section. (b) $T = \frac{1}{2}$ elastic cross section. (c) Cosine series expansion coefficients in the barycentric system. (d) Forward scattering cross section in the barycentric system.

analysis, and the Monte Carlo probabilities, are displayed in Fig. 2(a). The errors shown are a combination of statistical counting errors, scanning statistics, and our estimates of the uncertainties in background subtractions and beam contamination.

The charge-exchange cross section shows a broad shoulder at approximately 600 MeV corresponding to the second maximum in the π^-p elastic cross section and a well-defined peak at approximately 900 MeV corresponding to the third pion-nucleon resonance. This curve is in agreement with the Saclay counter results⁴ and with earlier bubble chamber results.⁵ The results are also tabulated in the first column of Table I.

Combining our data with the available information on the elastic cross sections,⁶ we extract the $T = \frac{1}{2}$ elastic cross section using the relationship $\sigma_{el}(T = \frac{1}{2}) = \frac{2}{3}[\sigma_{el}(\pi^-p) + \sigma(\pi^0n) - \frac{1}{3}\sigma_{el}(\pi^+p)]$. This is shown in Fig. 2(b) and is also in good agreement with the Saclay results.⁴ A fairly reliable interpolation on our data has been made at the points shown with error bars. The π^+ and π^- data at these points are those of Helland *et al.*⁵ The smooth curve was generated using all the available data on π^+ and π^- elastic scattering,⁷ and the results of this experiment for the charge-exchange contribution.

For the angular distribution determination, those two-gamma events are selected whose opening angles lie between the kinematic minimum and 80° . This eliminates all η^0 decays and reduces the multiple-pion background relative to the charge-exchange sample. The remaining multiple-pion contamination is removed by a subtraction using the higher multiplicity events. Since we have made no attempt to determine the

energy of the gamma rays in this experiment there is an ambiguity in the direction of the parent π^0 which gives rise to each two-gamma event. We experimentally determine the angle bisector of the two-gamma events in the π^-p barycentric system and fit these bisector distributions with a series of Legendre polynomials with argument $\cos\theta_B$, where θ_B is the angle between the angle bisector and the incoming beam track in the barycentric system. The true angular distribution can be unambiguously obtained from the bisector distribution by a linear transformation of the coefficients. The shapes of the two distributions are very similar. The Legendre series is then transformed to the conventional cosine series expansion

$$\frac{d\sigma}{d\Omega_{\pi^0}} = \sum_{l=0}^{l_{\max}} a_l \cos^l \theta_{\pi^0}.$$

The fits were made for successive values of l_{\max} ranging from 0 to 10. The fit which was retained always had a probability exceeding 4% and a statistically significant value of the coefficient of the highest order Legendre polynomial. In addition, at each energy, the value of l_{\max} was not permitted to decrease below that required at lower energies.

Figure 3 shows the experimental bisector distributions after efficiency correction together with the best-fit curves corresponding to the π^0 angular distributions. Table I gives the set of coefficients a_l we obtain; they are displayed graphically in Fig. 2(c). The striking features of these curves are the absence of any distinctive features in the 600-MeV region and the rapid increase of a_5 and the corresponding large negative increase of a_3 to peaks in the 900-MeV region.

Table I. Charge-exchange cross sections and cosine series coefficients.

Kinetic energy	Charge-exchange						
	cross section (mb)	A_0 (mb/sr)	A_1 (mb/sr)	A_2 (mb/sr)	A_3 (mb/sr)	A_4 (mb/sr)	A_5 (mb/sr)
545	7.71±0.62	0.185±0.052	0.424±0.146	0.842±0.415	1.174±0.243	0.740±0.484	...
588	6.67±0.49	0.198±0.028	0.461±0.073	0.715±0.226	0.668±0.121	0.474±0.262	...
619	6.77±0.47	0.122±0.015	0.436±0.054	1.075±0.138	0.608±0.093	0.291±0.175	...
659	6.15±0.49	0.210±0.047	0.346±0.119	0.680±0.370	0.523±0.191	0.266±0.419	...
755	4.39±0.35	0.083±0.035	0.244±0.185	0.690±0.298	-2.490±0.838	0.182±0.353	2.951±0.775
827	5.79±0.41	0.120±0.020	0.494±0.105	0.760±0.165	-4.630±0.485	0.439±0.193	5.395±0.447
878	7.23±0.58	0.061±0.054	0.808±0.280	1.176±0.441	-6.679±1.311	0.609±0.522	7.636±1.222
916	5.18±0.36	0.123±0.019	0.692±0.105	0.230±0.176	-4.148±0.512	1.062±0.220	4.539±0.492
1003	3.14±0.19	0.156±0.024	0.823±0.134	-0.014±0.203	-4.002±0.587	0.492±0.242	3.718±0.541

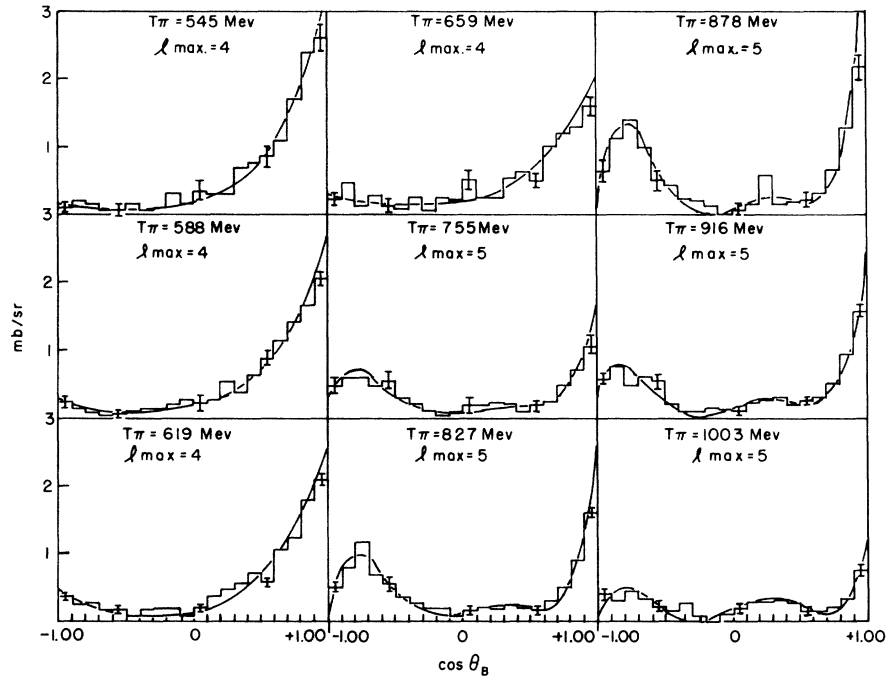


FIG. 3. Opening-angle bisector distributions.

This second fact is characteristic of the same $D_{5/2}$ - $F_{5/2}$ interference observed in this energy region in the elastic scattering.⁶

Combining our data with that of Helland *et al.*⁶ for the π^+p and π^-p elastic scattering, we can isolate the cosine series expansion coefficients corresponding to the $T = \frac{1}{2}$ elastic angular distribution. The same qualitative peaking is observed in the $T = \frac{1}{2}$ amplitudes and is strong evidence that both the $D_{5/2}$ and $F_{5/2}$ states involved are in the $T = \frac{1}{2}$ state. In particular, at the 900-MeV peak of the cross section the experimental $T = \frac{1}{2}$ angular distribution is given by

$$d\sigma/d\Omega(T = \frac{1}{2}) = [(0.25 \pm 0.11) + (2.65 \pm 1.15)x^2 + (9.07 \pm 3.06)x^4 + (2.97 \pm 2.57)x^6] + [(0.09 \pm 0.49)x - (19.69 \pm 2.44)x^3 + (32.54 \pm 3.07)x^5 + (1.65 \pm 1.31)x^7].$$

The errors quoted here come from the diagonal elements of the error matrices. It is appropriate to note, too, that the correlations are not negligible.

If the only states involved were $D_{5/2}$ and $F_{5/2}$, the angular distribution would be

$$d\sigma/d\Omega(T = \frac{1}{2}) \sim (|D_{5/2}|^2 + |F_{5/2}|^2)(1 - 2x^2 + 5x^4) + 2\text{Re}(D_{5/2}F_{5/2}^*)(5x - 26x^3 + 25x^5)$$

where $x = \cos\theta\pi_0$. A detailed quantitative comparison with the pure $D_{5/2}$ - $F_{5/2}$ angular distribution cannot be carried out, principally because of the presence of a small amount of other angular momentum states. However, it can be argued that the main features of the $T = \frac{1}{2}$ pion-nucleon interaction in this energy region are due to the dominant contribution from the $D_{5/2}$ - $F_{5/2}$ interference. Explicitly, if use is made of the experimental observation that the x^6 and x^7 coefficients are consistent with zero, then states higher than $J = \frac{5}{2}$ can be neglected and the large x^5 coefficient is solely due to $D_{5/2}$ - $F_{5/2}$ interference. The principal features of the coefficients in the experimental interference terms are that the x^5 and x^3 terms are large and opposite in sign as should be the case for pure $F_{5/2} + D_{5/2}$ states, and that the x^3 and x coefficients both deviate from the value expected for the pure case in a way consistent with the inclusion of a small amount of lower angular momentum states. We conclude that this may be taken as evidence that the $D_{5/2}$ and $F_{5/2}$ states provide the main contribution to the $T = \frac{1}{2}$ cross section at this energy. This conclusion does not support the conjecture of Kycia and Riley⁸ that the angular distribution in elastic π^-p scattering around 900 MeV is to be understood in terms of an interference between a $T = \frac{3}{2}$ $D_{5/2}$ state and a $T = \frac{1}{2}$ $F_{5/2}$ state.⁹

Finally, we plot in Fig. 2(d) the forward cross

section for charge exchange obtained from our data and compare it with the prediction using the forward dispersion relationships to calculate the real part and the optical theorem to calculate the imaginary part of the forward scattering amplitude. We used the most recent evaluation of the dispersion relation,¹⁰ based upon new Saclay measurements that have been published by Amblard *et al.*,¹¹ to make the prediction. The band around the predicted curve is the estimate of the uncertainty on the smooth curve as determined in reference 9. The agreement is seen to be quite good.

We would like to thank Mr. B. Dainese and his group, and Mr. Thomas Lyons and his group, for their expert assistance in the construction, development, and operation of the spark-chamber system. We would also like to thank the entire staff of the Brookhaven National Laboratory Cosmotron, without whose expert assistance and support the experiment could not have been performed. Finally, we are grateful to our respective scanning groups for their fast and efficient reduction of the data.

*Research performed partially at Brookhaven National Laboratory, Upton, New York.

†This work is supported in part through funds provided by the U. S. Atomic Energy Commission.

‡On leave of absence from the Weizmann Institute, Rehovoth, Israel.

¹C. Calvelli, P. Kusstatscher, L. Guerriero, C. F. Voci, F. Waldner, I. A. Pless, L. Rosenson, G. A. Salandin, F. Bulos, R. Lanou, and A. Shapiro, to be published.

²M. Chretien, F. Bulos, H. R. Crouch, Jr., R. E. Lanou, Jr., J. T. Massimo, A. M. Shapiro, J. A.

Averell, C. A. Bordner, Jr., A. E. Brenner, D. R. Firth, M. E. Law, E. E. Ronat, K. Strauch, J. C. Street, J. J. Szymanski, A. Weinberg, B. Nelson, I. A. Pless, L. Rosenson, G. A. Salandin, R. K. Yamamoto, L. Guerriero, and F. Waldner, *Phys. Rev. Letters* **9**, 127 (1962).

³C. A. Bordner, Jr., A. E. Brenner, and E. E. Ronat, Harvard University Internal Report (unpublished).

⁴J. C. Brisson *et al.*, *Proceedings of the Aix-en-Provence Conference on Elementary Particles, 1961* (C.E.N. Saclay, France, 1961), Vol. 1, p. 45; R. Turlay, thesis, University of Paris, 1963 (unpublished).

⁵A. Weinberg, A. E. Brenner, and K. Strauch, *Phys. Rev. Letters* **8**, 70 (1962); R. K. Yamamoto, thesis, Massachusetts Institute of Technology, 1963 (unpublished); H. R. Crouch, thesis, Brown University, 1964 (unpublished).

⁶J. A. Helland, T. J. Devlin, D. E. Hagge, M. J. Longo, B. J. Moyer, and C. D. Wood, *Phys. Rev. Letters* **10**, 27 (1963); also J. A. Helland *et al.*, *Phys. Rev.* **134**, B1062, B1079 (1964).

⁷For a summary of earlier results see P. Falk-Vairant and G. Valladas, *Rev. Mod. Phys.* **33**, 362 (1961); and R. Omnes and G. Valladas, *Proceedings of the Aix-en-Provence Conference on Elementary Particles, 1961* (C.E.N. Saclay, France, 1961), Vol. 1, p. 467.

⁸T. F. Kycia and K. F. Riley, *Phys. Rev. Letters* **10**, 266 (1963).

⁹R. H. Dalitz, private communication. This point was already made by Dalitz, using the data of R. K. Yamamoto, thesis, Massachusetts Institute of Technology, 1963 (unpublished).

¹⁰O. Guisan, thesis, University of Paris, 1964 (unpublished).

¹¹B. Amblard, P. Borgeaud, Y. Ducros, P. Falk-Vairant, O. Guisan, W. Laskar, P. Sonderegger, A. Stirling, M. Yvert, A. Tran Ha, and S. D. Warshaw, *Phys. Letters* **10**, 138 (1964).

VIOLATION OF CP INVARIANCE AND THE POSSIBILITY OF VERY WEAK INTERACTIONS*

L. Wolfenstein

Carnegie Institute of Technology, Pittsburgh, Pennsylvania

(Received 31 August 1964)

The observation¹ of the decay $K_2^0 \rightarrow 2\pi$ provides evidence that the weak interactions are not invariant with respect to the operation CP . The required magnitude of this CP -violating term in the weak-interaction Hamiltonian and the implications for other possible observations depend upon the theoretical model for explaining the $K_2^0 \rightarrow 2\pi$ decay. Sachs² has provided such a model in which (1) the CP -violating term is maximal in the sense that the $\Delta Q = -\Delta S$ decay interaction is 90° out of phase with $\Delta Q = +\Delta S$ interaction, (2) CP

violation would not occur in nonleptonic decays or in leptonic decays other than that of K^0 , and (3) the strength of the CP -violating term is comparable to the CP -conserving term. In this note we wish to raise some possible objections to the model of Sachs and to suggest an alternative which essentially satisfies conditions (1) and (2) above but requires that CP -violating weak interactions are weaker than the CP -conserving ones by a factor of 10^7 to 10^8 .

The Sachs model is equivalent to a weak inter-